Electronic Supplementary Information
for the communication entitled

Phospha-fluorescein Dye: A Red-Emissive Fluorescein Analogue with High Photobleaching Resistance

Aiko Fukazawa,*[1] Shinji Suda,[1] Masayasu Taki,*[2] Eriko Yamaguchi,[1] Marek Grzybowski,[2] Yoshikatsu Sato,[2] Tetsuya Higashiyama,[2,3] and Shigehiro Yamaguchi[1,2]*

[1]*Department of Chemistry, Graduate School of Science, Nagoya University, Furo, Chikusa, Nagoya 464-8602, Japan*
[2]*Institute of Transformative Bio-Molecules (WPI-ITbM), Nagoya University, Furo, Chikusa, Nagoya 464-8602, Japan*
[3]*Department of Biological Science, Graduate School of Science, Nagoya University, Furo, Chikusa, Nagoya 464-8602, Japan*

Contents

1. Experimental Details

General. Melting points (mp) or decomposition temperatures were determined with a Yanaco MP-S3 instrument (MP-S3). ^{1}H, ^{13}C{^{1}H}, and ^{31}P{^{1}H} NMR spectra were recorded with a JEOL AL-400 spectrometer (400 MHz for ^{1}H, 100 MHz for ^{13}C, and 162 MHz for ^{31}P), a JEOL JNM-ECS400 (400 MHz for ^{1}H, 100 MHz for ^{13}C, and 162 MHz for ^{31}P) or a JEOL A-600 spectrometer (600 MHz for ^{1}H and 150 MHz for ^{13}C) in $CDCl_3$, CD_2Cl_2, or CD_3OD. The chemical shifts in ^{1}H NMR spectra are reported in δ ppm using the residual protons of the solvents as an internal standard ($CHCl_3$ δ 7.26, CH_2Cl_2 δ 5.32, and CD_3OD δ 3.31), and those in ^{13}C NMR spectra are reported using the solvent signals as an internal standard ($CDCl_3$ δ 77.16, CD_2Cl_2 δ 53.84 and CD_3OD δ 49.0). The chemical shifts in ^{31}P NMR spectra are reported using H_3PO_4 (δ 0.00) as an external standard. Mass spectra were measured with a Bruker micrOTOF Focus spectrometry system with the ionization method of APCI or a Thermo Fisher Scientific Exactive with the ionization method of ESI. Thin layer chromatography (TLC) was performed on glass plates coated with 0.25 mm thickness of silica gel $60F_{254}$ (Merck). Column chromatography was performed using neutral silica gel PSQ100B (Fuji Silysia Chemicals) or silica gel 60 (Kanto Chemicals). Recycling preparative HPLC was performed using YMC LC-forte/R equipped with reversed phase column (YMC-Actus Triart C18). All reactions were performed under a nitrogen atmosphere unless stated otherwise. Commercially available solvents and reagents were used without further purification unless otherwise mentioned. Anhydrous THF and CH_2Cl_2 were purchased from Kanto Chemicals and further purified by Glass Contour Solvent Systems. Bis(2-bromo-4-*N*,*N*-dillaylaminophenyl)methane (**1**),[1] TokyoGreen,[2] and TokyoMagenta[1] were synthesized according to the literatures.

Compound 2. To a solution of bis[2-bromo-4-(*N*,*N*-diallylamino)phenyl]methane **1** (0.978 g, 1.89 mmol) in anhydrous THF (9 mL) was added *sec*-BuLi in cyclohexane and hexane (0.99 M, 4.00 mL, 3.96 mmol) at –78 °C for 5 min. After stirring for 1 h, $PhPCl_2$ (0.290 mL, 0.383 g, 2.14 mmol) was added over 10 min. After stirring at the same temperature for 3 h, the solution was warmed to 0 °C, and a 30% H_2O_2 aqueous solution (1.0 mL) was added. The mixture was stirred for 1 h, and then quenched with a Na_2SO_3 aqueous solution. The resulting solution was extracted with AcOEt. The combined organic layer was washed with brine, dried over anhydrous Na_2SO_4, and filtered. After removal the volatiles under the reduced pressure, the resulting solids were subjected to silica gel column chromatography (20/1 CH_2Cl_2/MeOH as an eluent, R_f= 0.40) to afford 0.257 g (0.525 mmol, 28%) of **2** as yellow liquid. ^{1}H NMR (400 MHz, CD_2Cl_2): δ 7.46–7.32 (m, 7H), 7.20 (dd, J = 8.4, 6.0 Hz, 2H), 6.82 (dd, J = 8.4, 2.8 Hz, 2H), 5.93–5.84 (m, 4H) 5.20–5.15 (m, 8H), 4.04–3.95 (m, 8H), 3.85 (dd, J = 18.4, 1.6 Hz, 1H), 3.65 (dd, J = 18.4, 3.6 Hz, 1H). ^{13}C{^{1}H} NMR (100 MHz, $CDCl_3$): δ 147.5 (d, J_{CP}= 13.3 Hz, C), 134.7 (d, J_{CP} = 104.1 Hz, C), 133.7 (s, CH), 131.1 (d, J_{CP} = 2.5 Hz, CH), 130.9 (d, J_{CP} = 9.9 Hz, CH), 129.8 (d, J_{CP} = 100.1 Hz, C), 129.3 (d, J_{CP} = 8.3 Hz, C), 129.0 (d, J_{CP} = 11.5 Hz, CH), 128.4 (d, J_{CP} = 12.4 Hz, CH), 116.4 (s, CH_2), 115.8 (s, CH), 114.2 (d, J_{CP} = 8.2 Hz, CH), 52.9 (s, CH_2), 35.3 (d, J_{CP} = 9.1 Hz, CH_2). ^{31}P{^{1}H} NMR (162 MHz, $CDCl_3$): δ 14.3. HRMS (ESI): *m*/*z* calcd. for $C_{31}H_{33}N_2NaOP$: 503.2228 ([M+Na]$^+$); found. 503.2224.

Diamino-PO-xanthone 4. To a solution of **2** (5.37 g, 11.2 mmol) in CH_2Cl_2 (112 mL) was added chloranil (8.26 g, 33.6 mmol) in air. The mixture was stirred for 3 h, and then quenched with a Na_2SO_3 aqueous solution. The resulting solution was extracted with CH_2Cl_2. The combined organic layer was washed with brine, dried over anhydrous Na_2SO_4, and filtered. After removing the solvents under the reduced pressure, the resulting mixture was subjected to silica gel column chromatography (20/1 CH_2Cl_2/MeOH as an eluent, R_f = 0.40) to afford 4.39 g of **3** as yellow solid, which still contained inseparable impurity, yet used in the next transformation without further purification.

Thus, to a solution of **3** (4.39 g) in degassed 1,2-dichloroethane (370 mL) was added $Pd(PPh_3)_4$ (1.34 g, 1.16 mmol) and 1,3-dimethylbarbituric acid (6.39 g, 40.9 mmol). The mixture was stirred at 80 °C for 24 h. $Pd(PPh_3)_4$ (1.34 g, 1.16 mmol) and 1,3-dimethylbarbituric acid (6.39 g, 40.9 mmol) were further added to the mixture in order to complete the reaction. After stirring at 80 °C for another 23 h, all the volatiles were removed under the reduced pressure. The resulting orange solid was subjected to silica gel column chromatography (10/1 $CHCl_3$/MeOH, R_f = 0.30) to afford 2.39 g (7.15 mmol, 64%) of **4** as yellow solids.

3: ^1H NMR (400 MHz, $CDCl_3$): δ 8.27 (dd, J = 9.0 Hz, 6.2 Hz, 2H), 7.59–7.54 (m, 2H), 7.39–7.32 (m, 3H), 7.14 (dd, J = 15 Hz, 2.6 Hz, 2H), 6.86 (dd, J = 9.0 Hz, 2.6 Hz, 2H), 5.82–5.74 (m, 4H), 5.15–5.09 (m, 8H), 4.08–3.93 (m, 8H). $^{31}P\{^1H\}$ NMR (162 MHz, $CDCl_3$): δ 7.0. HRMS (ESI): m/z calcd. for $C_{31}H_{31}NaN_2O_2P$: 517.2021 ([M+Na]$^+$); found. 517.2013.

4: Mp: 151 °C (dec.). ^1H NMR (400 MHz, CD_3OD): δ 8.15 (dd, J = 8.8 Hz, 6.0 Hz, 2H), 7.60–7.42 (m, 5H), 6.99 (dd, J = 14.8 Hz, 2.2 Hz, 2H), 6.91 (dd, J = 8.8 Hz, 2.2 Hz, 2H). The signal corresponding to NH_2 moiety was not observed. $^{13}C\{^1H\}$ NMR (100 MHz, CD_3OD): δ 181.4 (d, J_{CP} = 9.0 Hz, C), 154.8 (d, J_{CP}=13.3 Hz, C), 135.1 (d, J_{CP} = 97.6 Hz, C), 134.5 (d, J_{CP} = 108.3 Hz, C), 133.3 (d, J_{CP} = 2.5 Hz, CH), 132.6 (d, J_{CP} = 10.7 Hz, CH), 131.6 (d, J_{CP} = 10.7 Hz, CH), 129.9 (d, J_{CP} = 13.3 Hz, CH), 125.7 (d, J_{cp} = 6.6 Hz, C), 118.6 (s, CH), 115.3 (d, J_{CP} = 7.4 Hz, CH). $^{31}P\{^1H\}$ NMR (162 MHz, CD_3OD): δ 7.8. HRMS (APCI): m/z calcd. for $C_{19}H_{16}N_2O_2P$: 335.0944 ([M+H]$^+$); found. 335.0947.

Dihydroxy-PO-xanthone 5. To a solution of **4** (247 mg, 0.739 mmol) in 96% H_2SO_4 (2.5 mL) was added $NaNO_2$ (171 mg, 2.48 mmol) at 0 °C in air. After stirring for 3 h, the mixture was slowly poured to ice and stirred at 110 °C for 0.5 h. The resulting precipitate was collected by filtration, washed with distilled water, and dispersed in methanol. The resulting dark brown precipitates were filtered off, and the filtrate was concentrated under the reduced pressure to give 158 mg (0.470 mmol, 64%) of **5** as yellow solids. Mp: > 300 °C. ^1H NMR (400 MHz, CD_3OD): δ 8.33 (dd, J = 8.8, 6.0 Hz, 2H), 7.59–7.45 (m, 5H), 7.21 (dd, J = 14.2, 2.4 Hz, 2H), 7.16 (dd, J = 8.8, 2.4 Hz, 2H). The signal corresponding to the OH moiety was not observed. $^{13}C\{^1H\}$ NMR (100 MHz, CD_3OD): δ 181.5 (d, J_{CP} = 9.1 Hz, C), 164.0 (d, J_{CP} = 13.2 Hz, C), 135.6 (d, J_{CP} = 97.5 Hz, C), 133.7 (d, J_{CP} = 3.3 Hz, CH), 133.6 (d, J_{CP} = 109.9 Hz, C), 133.3 (d, J_{CP} = 10.7 Hz, CH), 131.7 (d, J_{CP} = 10.7 Hz, CH), 130.2 (d, J_{CP} = 12.3 Hz, CH), 129.1 (d, J_{CP} = 7.4 Hz, C), 121.6 (d, J_{CP} = 1.6 Hz, CH), 117.6 (d, J_{CP} = 6.6 Hz, CH). $^{31}P\{^1H\}$ NMR (162 MHz, CD_3OD): δ 6.4. HRMS (APCI): m/z calcd. for $C_{19}H_{14}O_4P$: 337.0624 ([M+H]$^+$); found. 337.0640.

Bis(*t*-butyldimethylsiloxy)-PO-xanthone 6. To a solution of **5** (229 mg, 0.680 mmol) and imidazole (232 mg, 3.40 mmol) in anhydrous CH_2Cl_2 (25 mL) was added *t*-butylchlorodimethylsilane (512 mg, 3.40 mmol) in anhydrous CH_2Cl_2 (7 mL). After stirring for 3 h, water was added and the resulting two layers were separated. The aqueous layer was extracted with CH_2Cl_2. The combined organic layer was dried over anhydrous Na_2SO_4, and filtered. After removal of the volatiles under the reduced pressure, the resulting mixture was subjected to silica gel column chromatography (30/1 CH_2Cl_2/EtOAc as an eluent, $R_f = 0.53$) to afford 354 mg (0.627 mmol, 92%) of **6** as colorless oil. ^{1}H NMR (400 MHz, $CDCl_3$): δ 8.36 (dd, J = 8.8, 5.8 Hz, 2H), 7.59–7.53 (m, 2H), 7.46–7.36 (m, 5H), 7.10 (dd, J = 8.8, 2.4 Hz, 2H), 0.95 (s, 18H), 0.21 (s, 6H), 0.20 (s, 6H). ^{13}C NMR (100 MHz, $CDCl_3$): δ 181.1 (d, J_{CP} = 9.1 Hz, C), 160.6 (d, J_{CP} = 14.1 Hz, C), 135.6 (d, J_{CP} = 95.9 Hz, C), 133.6 (d, J_{CP} = 107.4 Hz, C), 132.1 (d, J_{CP} = 10.7 Hz, CH), 132.0 (d, J_{CP} = 2.5 Hz, CH), 130.8 (d, J_{CP} = 10.7 Hz, CH), 129.6 (d, J_{CP} = 6.6 Hz, C), 128.9 (d, J_{CP} = 12.3 Hz, CH), 124.3 (d, J_{CP} = 2.5 Hz, CH), 121.9 (d, J_{CP} = 6.6 Hz, CH), 25.7 (s, CH_3), 18.4 (s, C), –4.2 (s, CH_3), –4.3 (s, CH_3). ^{31}P{^{1}H} NMR (162 MHz, $CDCl_3$): δ 4.5. HRMS (ESI): *m*/*z* calcd. for $C_{31}H_{41}NaO_4PSi_2$: 587.2179 ([*M*+Na]$^+$); found. 587.2167.

Phospha-fluorescein (POF). To a solution of 2-bromotoluene (89 μL, 0.74 mmol) in anhydrous THF (3 mL) was added *sec*-BuLi (0.99 M in cyclohexane and hexane, 0.90 mL, 0.89 mmol) at –78 °C. The mixture was stirred at –78 °C for 2 h and a solution of **6** (139 mg, 0.246 mmol) in anhydrous THF (3 mL) was slowly added. The reaction mixture was allowed to warm to room temperature and stirred for 1.5 h. Then, the reaction was quenched by the addition of 0.5 M hydrochloric acid (20 mL). After vigorously stirring for 45 min, the mixture was diluted with water and CH_2Cl_2. The layers were separated and the aqueous layer was extracted with CH_2Cl_2 five times. The combined organic layers were washed with brine and dried over Na_2SO_4. After filtration, the volatiles were removed under the reduced pressure, and the resulting mixture was dissolved in CH_2Cl_2 (10 mL). To this yellow solution, *p*-toluenesulfonic acid monohydrate (47 mg, 0.25 mmol) was added and the resulting mixture was stirred at room temperature for 45 min in order to complete the dehydroxylation. The obtained deep red solution was directly subjected to silica gel column chromatography (95/5 CH_2Cl_2/MeOH). After removal of the eluent under the reduced pressure, red oil was obtained which spontaneously solidified after the addition of toluene. The suspension was cooled to 0 °C and the precipitates were collected by filtration and dried under vacuum to give crude **POF** as bright red solids, which was further purified using reversed-phase HPLC (20/80 to 100/0 CH_3CN/H_2O containing 5 mM ammonium carbonate as eluents) to give **POF** (34 mg, 0.083 mmol, 34%) as brown powder. Mp. > 300 °C. ^{1}H NMR (400 MHz, CD_3OD): δ 7.76–7.36 (m, 8H), 7.27–7.13 (m, 3H), 7.03–6.94 (m, 2H), 6.58 (d, J = 9.5 Hz, 2H), 2.12 and 2.06 (two singlets, 3H, tolyl-methyl group signals from two diastereoisomers). ^{13}C NMR (100 MHz, CD_3OD): δ 140.0 (CH), 140.0 (CH), 138.3 (C), 138.2 (C), 137.9 (C), 137.7 (C), 137.6 (C), 137.3 (C), 137.2 (C), 137.1 (C), 134.1 (CH), 131.6 (CH), 131.6 (CH), 131.5 (CH), 131.4 (CH), 130.8 (CH), 130.5 (CH), 130.4 (CH), 130.4 (CH), 130.3 (CH), 129.9 (CH), 129.1 (CH), 127.2 (CH), 127.1 (CH), 125.9 (C), 125.8 (C), 125.7 (C), 125.3 (CH), 19.7 (CH_3), 19.6 (CH_3). ^{31}P{^{1}H} NMR (162 MHz,

$CDCl_3$): δ 11.1, 11.0. HRMS (ESI): *m*/*z* calcd. for $C_{26}H_{19}NaO_3P$: 433.0970 ([*M*+Na]$^+$); found. 433.0960.

Scheme S1. Synthesis of **AcPOF**

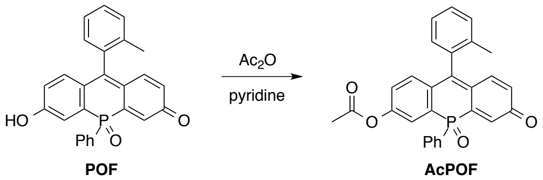

Acetyl-protected POF (AcPOF). POF (37 mg, 0.090 mmol) was dissolved in 5 mL of dry pyridine under a nitrogen atmosphere. Acetic anhydride (85 μL, 0.90 mmol) was added and the mixture was stirred for 3 h at room temperature. Solvents were removed under the reduced pressure and the product was purified by silica gel column chromatography (3/1 to 2/1 CH_2Cl_2/AcOEt) and further recrystallized from CH_2Cl_2/hexane to give **AcPOF** (33 mg, 0.073 mmol, 81%) as yellow powder. Mp. 175–179 °C. ^{1}H NMR (400 MHz, CD_2Cl_2): δ 7.75–7.60 (m, 3H), 7.60–7.52 (m, 1H), 7.52–7.30 (m, 5H), 7.30–7.06 (m, 3H), 7.06–6.91 (m, 2H), 6.26 (dd, J = 9.8, 1.8 Hz, 1H), 2.26 (s, 3H), 2.13 and 2.08 (two singlets, 3H, tolyl-methyl group signals from two diastereoisomers). ^{13}C NMR (150 MHz, CD_2Cl_2): δ 184.3 (s, C), 184.2 (s, C), 168.9 (s, C), 153.0 (d, J_{CP} = 14.4 Hz, C), 150.6 (d, J_{CP} = 7.2 Hz, C), 150.5 (d, J_{CP} = 10.1 Hz, C), 140.7 (d, J_{CP} = 90.5 Hz, C), 140.33 (d, J_{CP} = 90.5 Hz, CH), 139.7 (d, J_{CP} = 10.1 Hz, CH), 139.62 (d, J_{CP} = 8.6 Hz, CH), 137.2 (s, C), 137.2 (d, J_{CP} = 4.4 Hz, CH), 137.0 (d, J_{CP} = 2.9 Hz, CH), 136.5 (s, C), 136.4 (s, C), 136.4 (s, C), 135.0 (d, J_{CP} = 5.9 Hz, C), 134.9 (d, J_{CP} = 5.7 Hz, C), 134.3 (d, J_{CP} = 11.6 Hz, CH), 134.3 (d, J_{CP} = 10.1 Hz, CH), 133.7 (d, J_{CP} = 102.0 Hz, C), 133.5 (d, J_{CP} = 107.7 Hz, C), 133.0 (d, J_{CP} = 89.1 Hz, C), 132.9 (s, CH), 131.0 (s, CH), 130.8 (d, J_{CP} = 10.1 Hz, CH), 130.8 (d, J_{CP} = 11.4 Hz, CH), 130.3 (s, CH), 129.62 (CH), 129.61 (CH), 129.51 (CH), 129.46 (CH), 129.42 (CH), 129.39 (CH), 129.38 (d, J_{CP} = 8.6 Hz, C), 129.2 (s, CH), 127.73 (d, J_{CP} = 5.9 Hz, C), 126.62 (s, CH), 126.59 (s, CH), 126.56 (s, CH), 125.94 (d, J_{CP} = 5.7 Hz, CH), 125.87 (d, J_{CP} = 7.2 Hz, CH), 21.2 (s, CH_3), 19.8 (s, CH_3). ^{31}P{^{1}H} NMR (162 MHz, $CDCl_3$): δ 5.8, 5.7. HRMS (ESI): *m*/*z* calcd. for $C_{28}H_{21}NaO_4P$: 475.1075 ([*M*+Na]$^+$); found. 475.1066.

X-ray Data Collection of POF. Block-shaped red single crystals were grown by slow diffusion of hexanes into a $CHCl_3$ solution of POF. Intensity data were collected at 123 K on a Rigaku Single Crystal X-ray diffractometer equipped with FR-X generator, Varimax optics, and PILATUS 200K photon counting detector with MoKα radiation (λ = 0.71075 Å). A total of 19043 reflections were measured with the maximum 2θ angle of 50.0°, of which 4694 were independent reflections (R_{int} = 0.0195). The structure was solved by direct methods (SIR-2003) and refined by the full-matrix least-squares on F^2 (SHELXL-2013).[3] *o*-Tolyl group are disordered and solved using appropriate disordered models. Two sets of *o*-tolyl groups, *i.e.*, (C20, C21, C22, C23, C24, C25, C26) and (C27, C28, C29, C30, C31, C32, C33) were placed and their occupancies were refined to be 0.55 and 0.45, respectively. All non-hydrogen atoms were refined anisotropically and all hydrogen atoms were placed using AFIX instructions. The crystal data are as follows: $C_{26}H_{19}O_3P$; FW = 410.38, crystal size 0.30 × 0.30 × 0.10 mm^3, monoclinic, *C*2/*c*, *a* = 16.295(13) Å, *b* = 14.157(18) Å, *c* = 18.637(17) Å, β

= 104.42(2)°, V = 4164(7) Å^3, Z = 8, D_c =1.309 g cm^{-3}, μ = 0.157 mm^{-1}, R_1 = 0.0402 ($I > 2\sigma(I)$), wR_2 = 0.1095 (all data), GOF = 1.063. CCDC 1435421 contains the supplementary crystallographic data for this compound. This data can be obtained free of charge from The Cambridge Crystallographic Data Centre at www.ccdc.cam.ac.uk/data_request/cif.

2. Computational Method and Results

Computational Method. The geometry optimization of the deprotonated forms of TokyoGreen, TokyoMagenta, and POF were performed using the B3LYP functional[4] with the 6-31G(d,p) basis set,[5] implemented in the Gaussian 09 program.[6] Stationary points in the lowest singlet state (S_0) were optimized without any symmetry assumptions and characterized by frequency analysis at the same level of theory (the number of imaginary frequencies, NIMAG, was 0). The Cartesian coordinates for these compounds are given in Tables S1–3.

Table S1. Cartesian Coordinates (Å) of the Optimized Structures for TokyoGreen in S_0 (charge = –1)

atom	*x*	*y*	*z*
C	1.21990835	-0.38380422	-0.12288088
C	0.00003362	0.31751772	-0.15049718
C	-1.22011743	-0.38331093	-0.1226561
C	-1.20203636	-1.81890191	-0.05574537
C	1.20126407	-1.81938453	-0.05595358
C	2.34223025	-2.58049294	-0.01737638
H	2.2729308	-3.66303409	0.03229608
C	-2.34330481	-2.57954776	-0.01699002
C	-3.65867325	-1.97021797	-0.03898645
H	-2.274439	-3.66211722	0.03266607
C	3.65784132	-1.9716947	-0.03959409
O	-0.00051861	-2.48578775	-0.02637957
C	-2.51691062	0.22930866	-0.14605892
C	-3.66797928	-0.50606735	-0.10670749
H	-2.56857617	1.3144231	-0.19930877
H	-4.64297609	-0.02468538	-0.12654761
C	2.5169457	0.2282886	-0.1465592
C	3.6677242	-0.50755239	-0.10740463
H	2.56904723	1.31337914	-0.19986627
H	4.64291229	-0.02656689	-0.12746781
O	-4.72180564	-2.63732201	-0.0028201
O	4.72071117	-2.63922991	-0.00367361
C	0.00033925	1.81543755	-0.20998746
C	0.00097645	4.61942457	-0.39826608
C	0.0003429	2.4525021	-1.45877482
C	0.00065122	2.59333277	0.96906054
C	0.00097046	3.99063125	0.84975816
C	0.00065911	3.8460165	-1.56045789
H	0.00010211	1.8404603	-2.357506
H	0.00122378	4.59510273	1.75516992
H	0.00065904	4.31960262	-2.53947732
H	0.0012284	5.70557804	-0.45950847
C	0.00062708	1.94233045	2.33360072
H	0.00101491	2.69817502	3.12683612
H	0.88060213	1.30243246	2.47015231
H	-0.87977805	1.30307466	2.4704106

Table S2. Cartesian Coordinates (Å) of the Optimized Structures for TokyoMagenta in S_0 (charge = –1)

atom	*x*	*y*	*z*
C	-0.02377047	1.28389446	-0.11839708
C	-0.64933291	0.00029373	-0.14813637
C	-0.0246843	-1.28375187	-0.11849558
C	1.41058648	-1.48093158	-0.05118382
C	1.4116423	1.48004338	-0.05111224
C	1.93930063	2.75030006	-0.00108909
H	3.01745107	2.90536709	0.05061173
C	1.93733856	-2.75156654	-0.00123886
C	1.13664409	-3.97147902	-0.01294903
H	3.01537698	-2.9074019	0.05047398
C	1.13947571	3.97078426	-0.01270749
Si	2.56133978	-0.00085266	-0.04665643
C	-0.82611692	-2.48059853	-0.1387017
C	-0.29537218	-3.74242583	-0.0878889
H	-1.90630114	-2.3833206	-0.19663082
H	-0.94009547	-4.61883287	-0.10485821
C	-0.82435278	2.4813114	-0.13847977
C	-0.29270609	3.74275639	-0.08758882
H	-1.90460854	2.38480763	-0.19636135
H	-0.93680679	4.61962314	-0.10445173
O	1.64963481	-5.11657579	0.03634255
O	1.65328223	5.11551092	0.03669103
C	-2.15781189	0.00082141	-0.21155023
C	-4.96448569	0.00173639	-0.41253711
C	-2.79185473	0.00141067	-1.46170529
C	-2.94312377	0.00068802	0.9625233
C	-4.34001699	0.00115586	0.83756142
C	-4.18464939	0.00186645	-1.57050375
H	-2.17628397	0.00151245	-2.35810712
H	-4.94788141	0.00106644	1.74087418
H	-4.65324182	0.00232253	-2.55209698
H	-6.05041147	0.00208948	-0.47851227
C	-2.30114855	-0.00008227	2.33117914
H	-3.06201996	0.00089921	3.11977286
H	-1.66153076	0.87959348	2.47093285
H	-1.66381264	-0.88142557	2.47096912
C	3.66894466	-0.00126235	-1.58894575
H	3.06261273	-0.00123762	-2.50264713
H	4.31271491	-0.89029075	-1.61244113
H	4.31312245	0.88746412	-1.6126553
C	3.67389964	-0.00125839	1.49082473
H	3.07175	-0.00090967	2.4072136
H	4.31912909	0.88667004	1.51171791
H	4.31831106	-0.88977688	1.51185092

Table S3. Cartesian Coordinates (Å) of the Optimized Structures for POF in S_0 (charge = –1)

atom	*x*	*y*	*z*
C	0.6485816	1.26716941	-0.27245424
C	1.23337716	-0.0002005	-0.00033187
C	0.64824066	-1.26740499	-0.27249052
C	-0.67086982	-1.42669746	-0.84234478
C	-0.67048024	1.42684569	-0.84230869
C	-1.15790215	2.65239981	-1.21681449
H	-2.14674084	2.74100586	-1.66057397
C	-1.15862428	-2.65210217	-1.21689899
C	-0.40051306	-3.89051076	-1.0434289
H	-2.14748192	-2.74042142	-1.66067279
C	-0.39943676	3.8905883	-1.04332886
P	-1.78693367	0.00023223	-1.00552629
C	1.38306138	-2.4869153	-0.06688564
C	0.90362778	-3.71870636	-0.42314122
H	2.37121935	-2.4241832	0.38029719
H	1.4945056	-4.6163812	-0.25570583
C	1.3837421	2.48646522	-0.06681494
C	0.9046503	3.71840128	-0.423033
H	2.37188112	2.42344209	0.38037334
H	1.49577569	4.61590678	-0.25556319
O	-0.85091564	-5.00522269	-1.39331208
O	-0.84953633	5.00544086	-1.39315601
C	2.62388155	-0.00036965	0.58119032
C	5.18390635	-0.00061237	1.74492423
C	2.78284039	-0.00063419	1.97352658
C	3.76774418	-0.00020155	-0.24831645
C	5.0335398	-0.00033099	0.3556504
C	4.05091413	-0.00076489	2.56010544
H	1.89505262	-0.00075518	2.6014418
H	5.91764878	-0.00020721	-0.27949427
H	4.14903239	-0.00098227	3.64322024
H	6.17909986	-0.00070626	2.18409637
C	3.64066955	0.00018149	-1.75439581
H	4.62772608	-0.00013218	-2.22970455
H	3.09097566	0.88055438	-2.10793549
H	3.09021273	-0.87954401	-2.10833867
O	-2.69983256	0.00033053	-2.20592016
C	-2.78227937	0.00034351	0.54769971
C	-4.40396804	0.00037101	2.83711773
C	-4.17769801	-0.00008292	0.42503147
C	-2.20337236	0.00079743	1.82522686
C	-3.01050197	0.00081144	2.96442118
C	-4.98550911	-0.00007383	1.56656982
H	-4.61381884	-0.00038399	-0.57017064
H	-1.12160482	0.00115336	1.93130933
H	-2.55275274	0.00117776	3.95121833
H	-6.06833037	-0.00040065	1.46177228
H	-5.03184949	0.00038454	3.72557876

3. Photophysical Properties

Photophysical measurements. UV-vis absorption spectra of **POF** were measured with a Shimadzu UV-3150 spectrometer with a resolution of 0.2 nm using 10^{-5} M sample solutions in aqueous buffer solutions (pH = 3–5.5: citric acid/Na_2HPO_4 aqueous solutions, pH = 6–8: Na_2HPO_4/NaH_2PO_4 aqueous solutions, pH = 9–11: Na_2CO_3/$NaHCO_3$ aqueous solutions) containing 1% DMSO in a 1 cm square quartz cuvette. Emission spectra were measured with a Hitachi F-4500 spectrometer with a resolution of 1 nm using 10^{-6} M sample solutions (Fig. 3, Table 1, and Fig. S1). Excitation spectra were measured with Horiba SPEX Fluorolog 3 spectrofluorometer equipped with a Hamamatsu PMA R5509-73 and a cooling system C9940-01 using 10^{-6} M sample solutions (Fig. S2). Absolute fluorescence quantum yields were determined with a Hamamatsu photonics PMA-11 calibrated integrating sphere system.

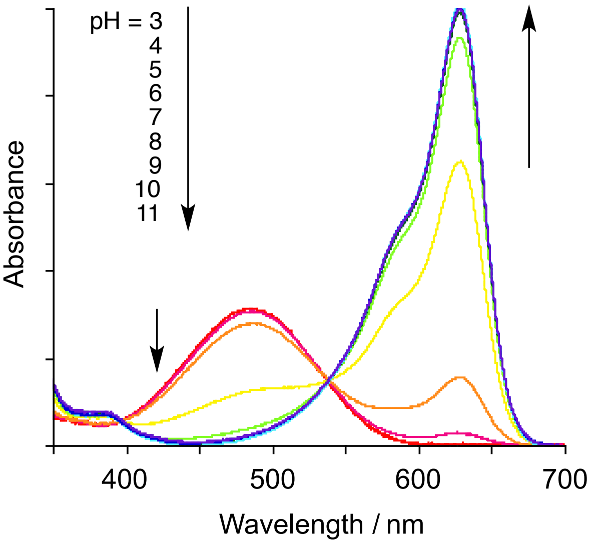

Figure S1. pH-dependent absorption spectra of POF in aqueous buffer solutions

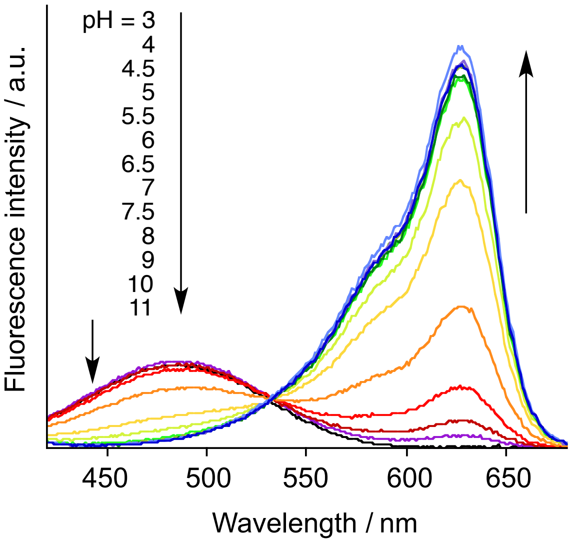

Figure S2. pH-dependent excitation spectra of POF.

Determination of Acid Dissociation Constant (K_a). Relative absorbances of POF at 627 nm (A_{627}) at various pH values were plotted against the pH values, and were analyzed by non-linear least square curve fitting using the following equation (eq. 1).

$$A_{627} = \frac{10^{-pH}A_0 + 10^{-pK_a}A_\infty}{10^{-pH} + 10^{-pK_a}} \qquad \text{(eq. 1)}$$

where A_0 and A_∞ represent the initial and final absorbance values at 627 nm, respectively.

The ratios of fluorescence intensity at 720 nm upon the excitation with two different excitation wavelengths 532 nm and 627 nm (I_{627}/I_{532}) were plotted against the pH values. The data was analyzed by curve fitting using the following equation (eq. 2):

$$I_{627}/I_{532} = \frac{R_{\min} + R_{\max}10^{-pK_a}10^{pH}s}{1 + 10^{-pK_a}10^{pH}s}, \quad s = \frac{S_{A^-}}{S_{AH}} \qquad \text{(eq.2)}$$

where R_{min} and R_{max} are the minimum and maximum ratio values, respectively. The expression s_{A-} and s_{AH} are the fluorescence intensity of the H$^+$-free and H$^+$-bound forms with 532 nm excitation.

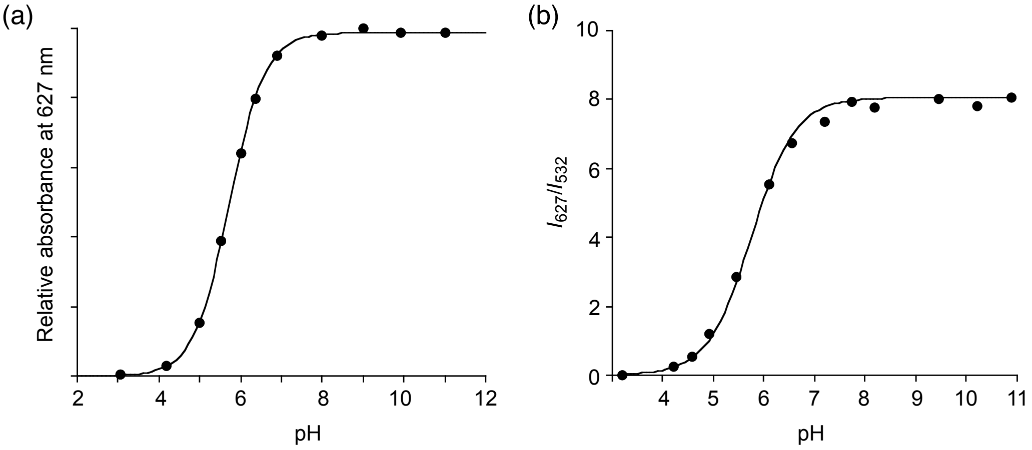

Figure S3. (a) The plots of absorbance at 627 nm (A_{627}) as a function of the pH value and their fitting curve (R^2 = 0.99984). (b) The plots of fluorescence intensity ratio between two different excitation wavelengths 532 nm and 627 nm (I_{627}/I_{532}) as a function of the pH value and their fitting curve (R^2 = 0.99691).

4. Biological Experiments

Cell incubation and imaging. HeLa (RIKEN Cell Bank, Japan) and RAW264.7 (JCRB cell bank, Japan) cells were cultured in Dulbecco's modified Eagle's medium (DMEM, Sigma) containing 10% fetal bovine serum (FBS, Gibco) and 1% Antibiotic-Antimycotic (AA, Sigma) at 37 °C in a 5% CO_2/95% air incubator. Two days before imaging, HeLa and RAW264.7 cells were seeded in 35 mm glass-bottom and 8-well glass-bottom dishes, respectively. For staining experiments, HeLa cells were incubated with 5 μM of AcPOF in PBS for 10 min at 37 °C and then rinsed twice with PBS. After replacement of medium to DMEM without phenol red, cells were imaged using Olympus FV10i confocal fluorescence microscope with an excitation laser of 635 nm. In case of RAW264.7 cells, on the other hand, DMEM containing 5 μM of AcPOF, 10 mM HEPES (pH 7.4), 1% DMSO, and 0.02% of Pluronic F-127 was used as the incubation medium. After cells were stained for 15 min at 37 °C and rinsed twice with DMEM, each well was filled with a pH calibration buffer of pH 4.5 or 6.5 (Thermo Fisher Scientific) containing 10 μM of valinomycin and 10 μM of nigericin. The cell images were acquired using TCS SP8 STED (Leica) with a HC PL APO 20x/0.75 IMM CORR CS2 lens. The cells were excited with a 627 nm (White Light Laser; 80 MHz, output power 70%, AOTF 50%) laser lines and the emission was recorded through a 485–527 nm and 635–750 nm filter.

Cytotoxicity evaluation. HeLa cells were seeded into a flat-bottomed 96-well plate (1×10^4 cells/well) and incubated in DMEM containing 10% FBS at 37 °C in a 5% CO_2/95% air incubator for 24 h. The medium was then replaced with culture medium containing various concentrations of AcPOF (1, 5, and 10 μM) and the cells were further incubated for 24 h at 37 °C. After removing the medium, MTT reagent (final concentration, 0.5 mg/mL) was added to each well, and the plates were incubated for another 4 h in a CO_2 incubator. Excess MTT tetrazolium solution was then removed and the cells were once washed with PBS. After the formazan crystals were solubilized in DMSO (100 μL/well) for 30 min at room temperature, the absorbance of each well was measured by SpectraMax i3 (Molecular Devices) at a wavelength of 535 nm.

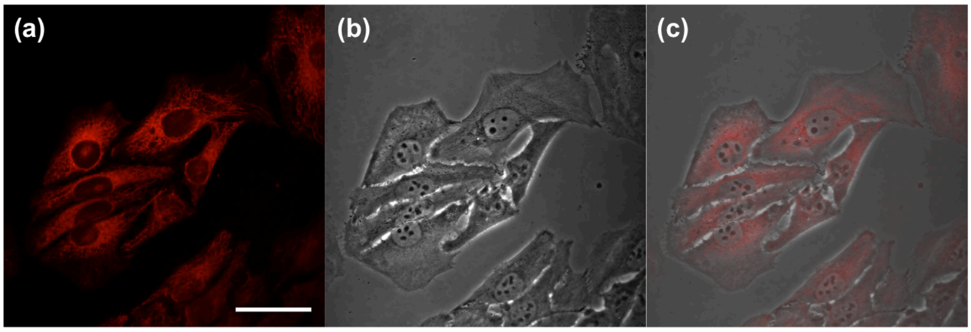

Figure S4. Fluorescence images of HeLa cells stained with 5 μM of AcPOF for 10 min at 37 ºC. (a) Confocal fluorescence image observed with an excitation at 633 nm, (b) bright field image, and (c) merged image of (a) and (b). Scale bar represents 50 μm.

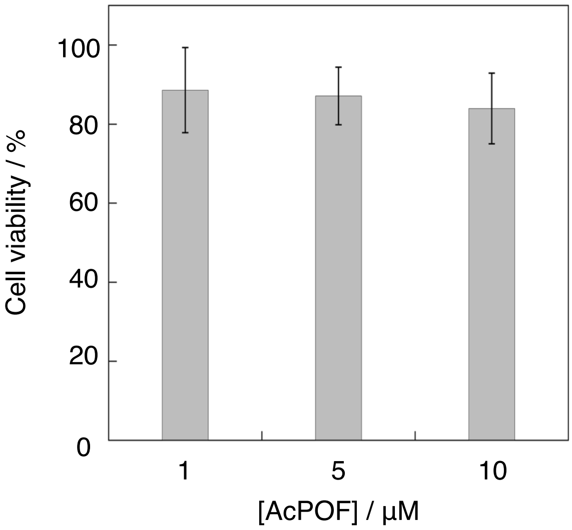

Figure S5. Cell viability results of the HeLa cells with **AcPOF** by MTT assay. The results are expressed as percentages of the dye-free controls. All data are presented as mean ± standard deviation (n = 12).

5. References

1 T. Egawa, Y. Koide, K. Hanaoka, T. Komatsu, T. Terai, T. Nagano, *Chem. Commun.*, 2011, **47**, 4162–4164.

2 Y. Urano, M. Kamiya, K. Kanda, T. Ueno, K. Hirose, T. Nagano, *J. Am. Chem. Soc.*, 2005, **127**, 4888–4894.

3 G. M. Sheldrick, *SHELX-2013, Program for the Refinement of Crystal Structures*; University of Gottingen: Gottingen, Germany, 2013.

4 (a) A. D. Becke, *Phys. Rev. A*, 1988, **38**, 3098–3100. (b) C. Lee, W. Yang, R. G. Parr, *Phys. Rev. B*, 1988, **37**, 785–789. (c) A. D. Becke, *J. Chem. Phys.*, 1993, **98**, 5648–5652.

5 (a) R. Ditchfield, W. J. Hehre, J. A. Pople, *J. Chem. Phys.*, 1971, **54**, 724–728. (b) W. J. Hehre, R. Ditchfield, J. A. Pople, *J. Chem. Phys.*, 1972, **56**, 2257–2261. (c) P. C. Hariharan, J. A. Pople, *Theor. Chim. Acta*, 1973, **28**, 213–222. (d) M. M. Francl, W. J. Pietro, W. J. Hehre, J. S. Binkley, M. S. Gordon, D. J. DeFrees, J. A. Pople, *J. Chem. Phys.*, 1982, **77**, 3654–3665.

6 Gaussian 09, Revision C.01, M. J. Frisch, G. W. Trucks, H. B. Schlegel, G. E. Scuseria, M. A. Robb, J. R. Cheeseman, G. Scalmani, V. Barone, B. Mennucci, G. A. Petersson, H. Nakatsuji, M. Caricato, X. Li, H. P. Hratchian, A. F. Izmaylov, J. Bloino, G. Zheng, J. L. Sonnenberg, M. Hada, M. Ehara, K. Toyota, R. Fukuda, J. Hasegawa, M. Ishida, T. Nakajima, Y. Honda, O. Kitao, H. Nakai, T. Vreven, J. A. Montgomery, Jr., J. E. Peralta, F. Ogliaro, M. Bearpark, J. J. Heyd, E. Brothers, K. N. Kudin, V. N. Staroverov, T. Keith, R. Kobayashi, J. Normand, K. Raghavachari, A. Rendell, J. C. Burant, S. S. Iyengar, J. Tomasi, M. Cossi, N. Rega, J. M. Millam, M. Klene, J. E. Knox, J. B. Cross, V. Bakken, C. Adamo, J. Jaramillo, R. Gomperts, R. E. Stratmann, O. Yazyev, A. J. Austin, R. Cammi, C. Pomelli, J. W. Ochterski, R. L. Martin, K. Morokuma, V. G. Zakrzewski, G. A. Voth, P. Salvador, J. J. Dannenberg, S. Dapprich, A. D. Daniels, O. Farkas, J. B. Foresman, J. V. Ortiz, J. Cioslowski, D. J. Fox, Gaussian, Inc., Wallingford CT, 2010.

6. NMR Spectra

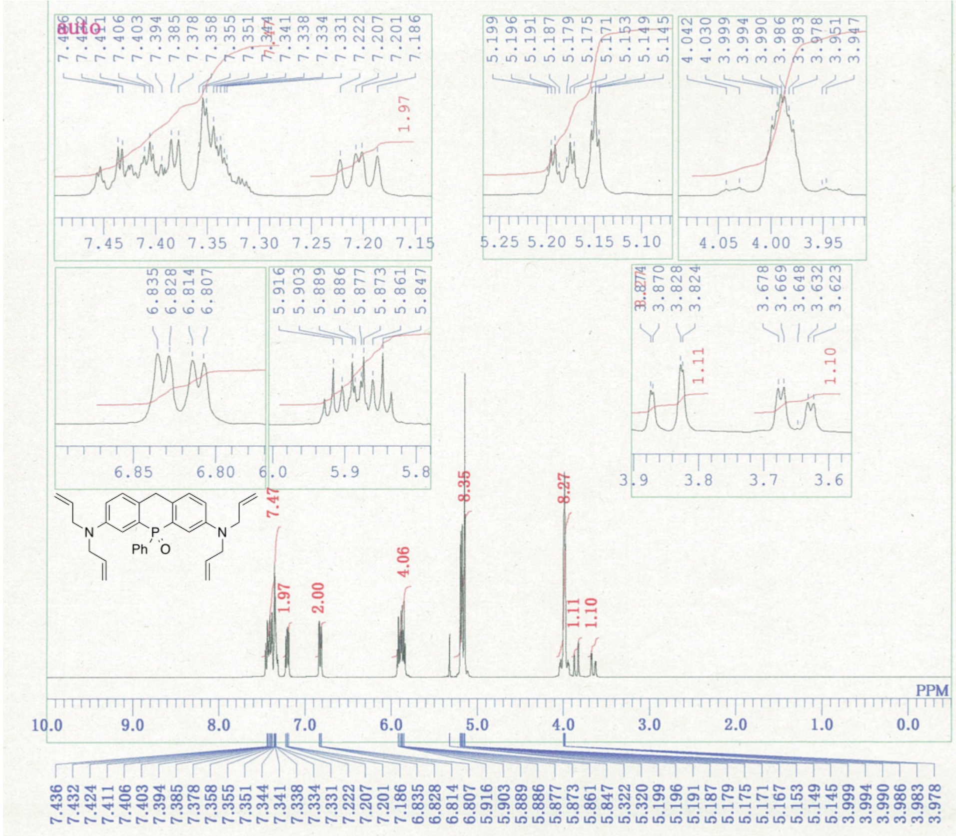

Figure S6. ^{1}H NMR spectrum of **2** (400 MHz, CD_2Cl_2).

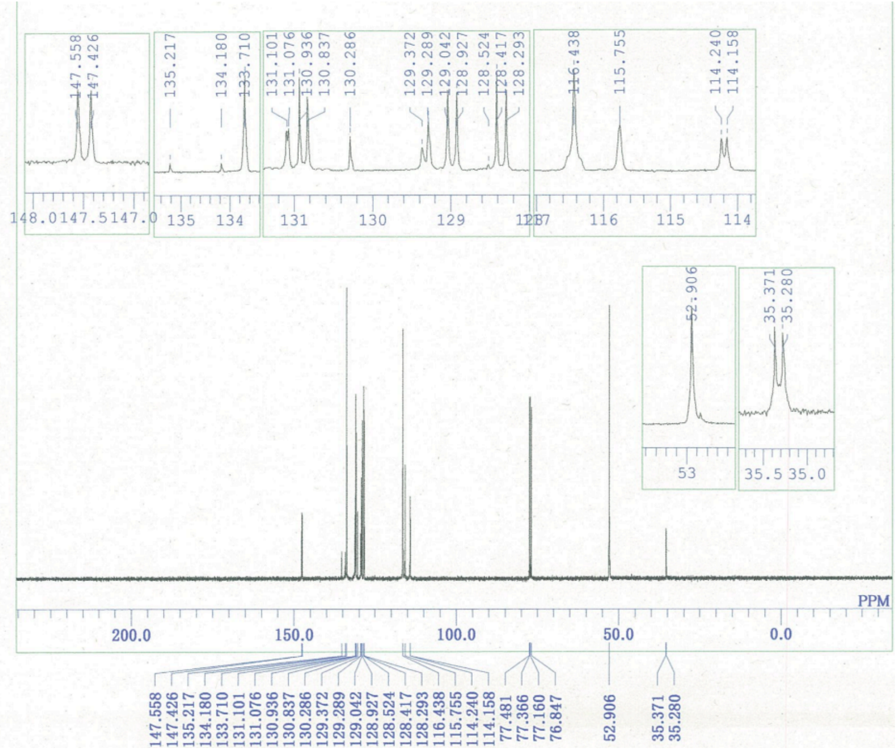

Figure S7. ^{13}C{^{1}H} NMR spectrum of **2** (100 MHz, $CDCl_3$).

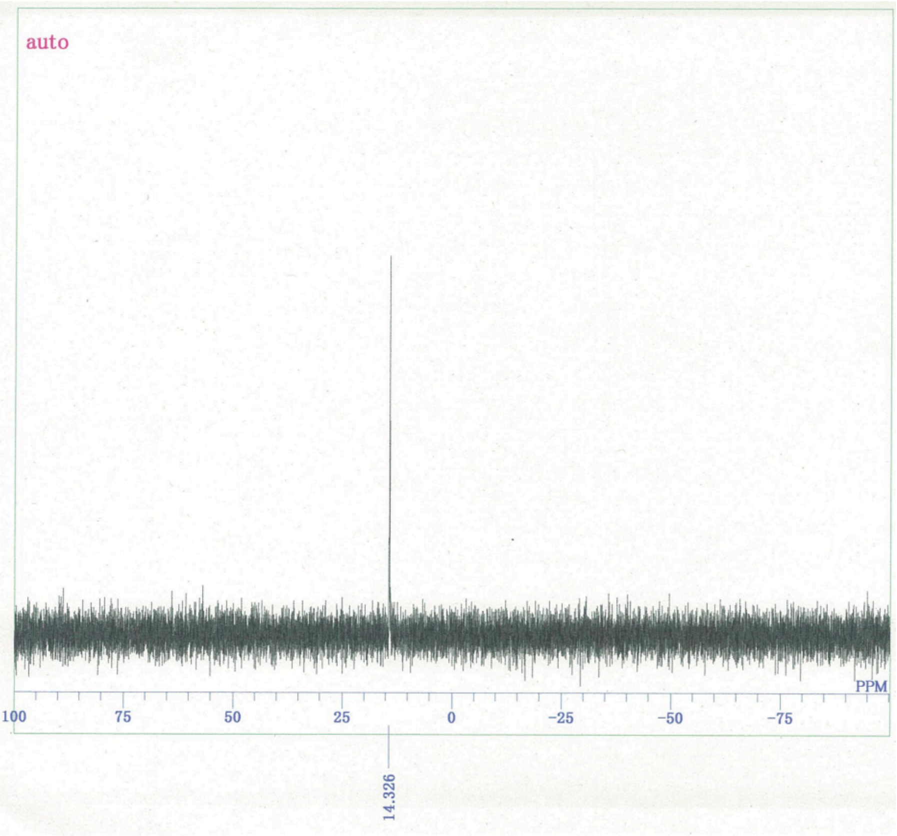

Figure S8. $^{31}P\{^{1}H\}$ NMR spectrum of **2** (162 MHz, $CDCl_3$).

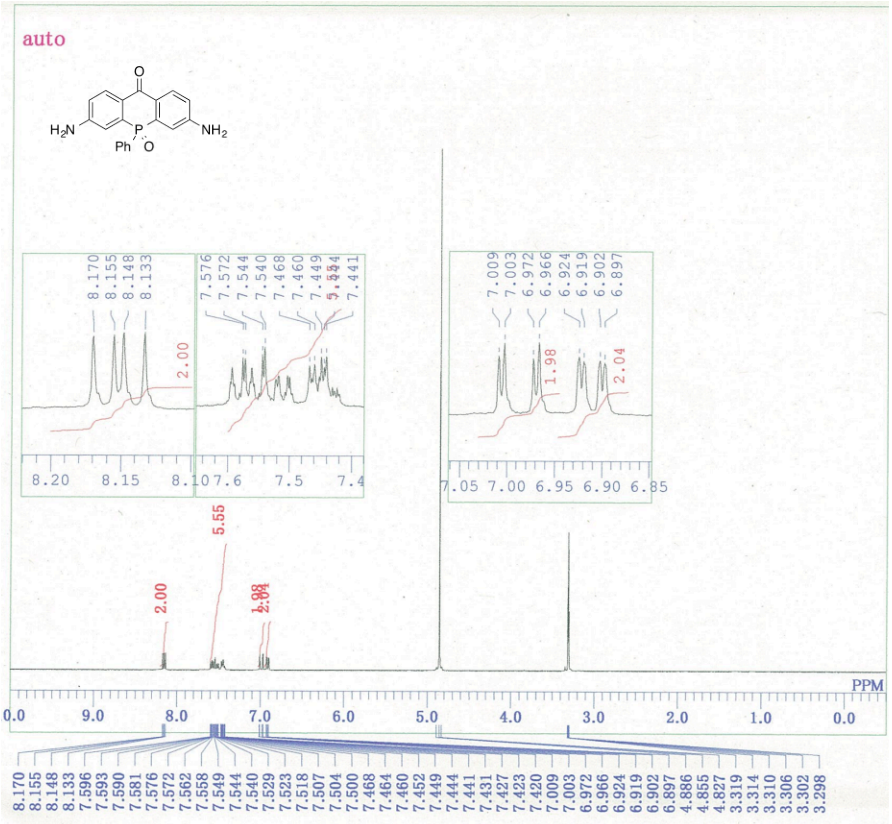

Figure S9. ^{1}H NMR spectrum of **4** (400 MHz, CD_3OD).

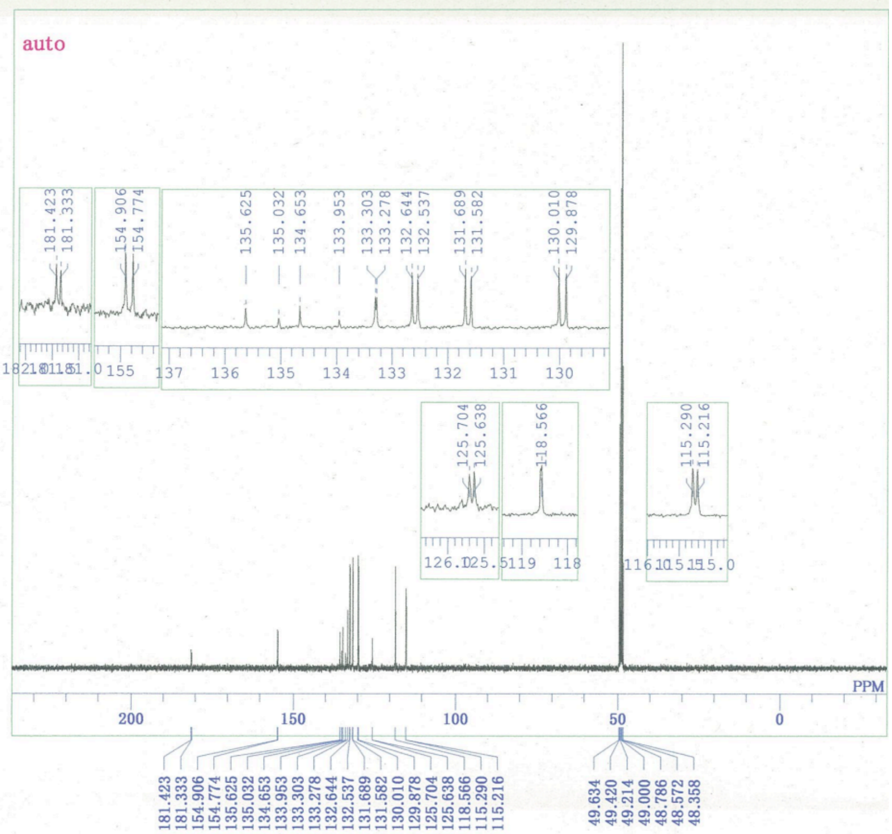

Figure S10. $^{13}C\{^1H\}$ NMR spectrum of **4** (100 MHz, CD_3OD).

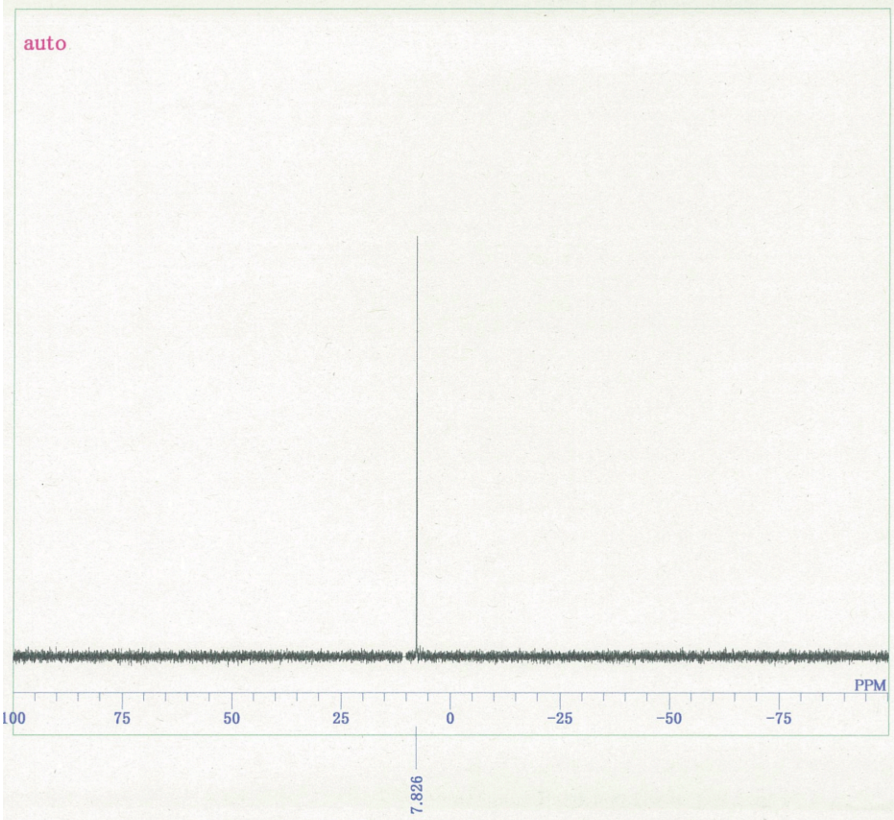

Figure S11. $^{31}P\{^1H\}$ NMR spectrum of **4** (162 MHz, CD_3OD).

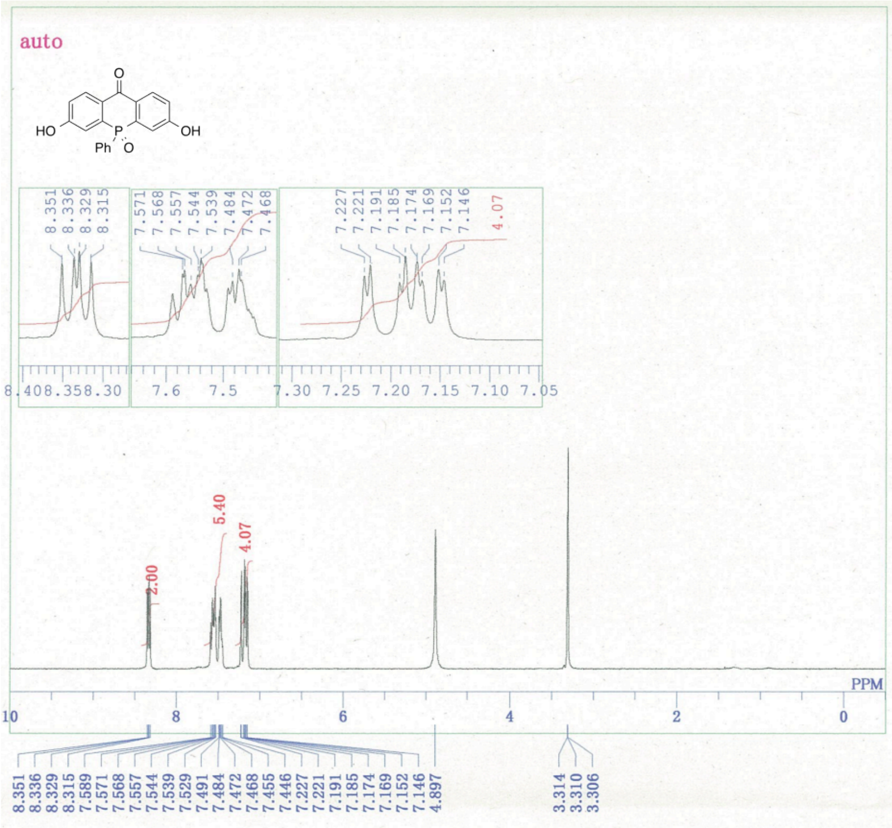

Figure S12. ^{1}H NMR spectrum of **5** (400 MHz, CD_3OD).

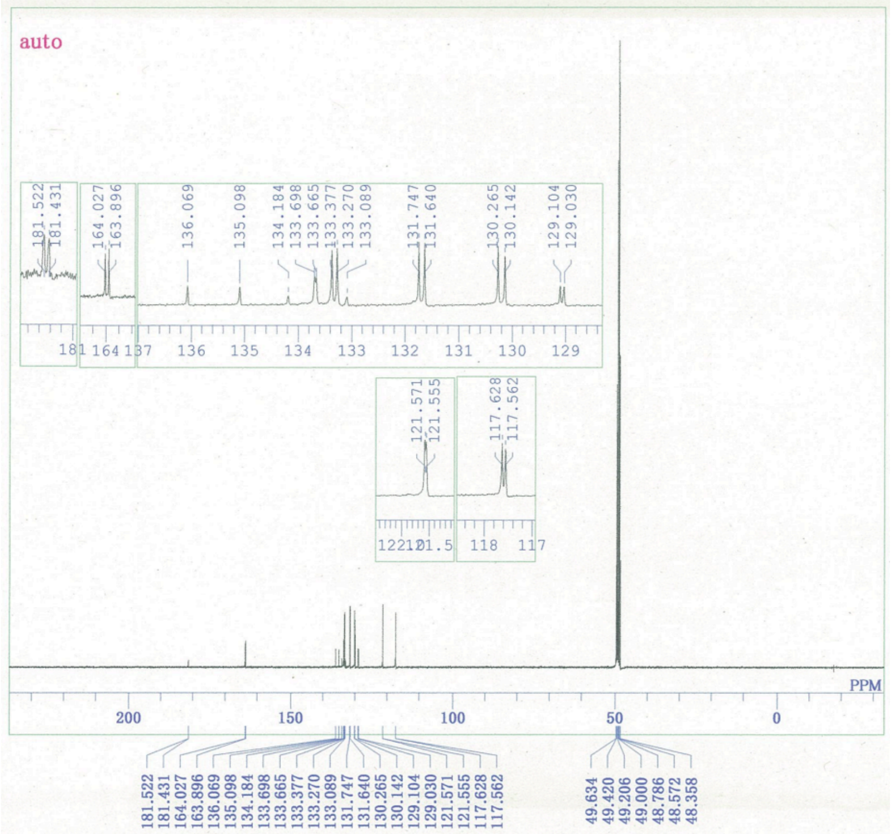

Figure S13. $^{13}C\{^1H\}$ NMR spectrum of **5** (100 MHz, CD_3OD).

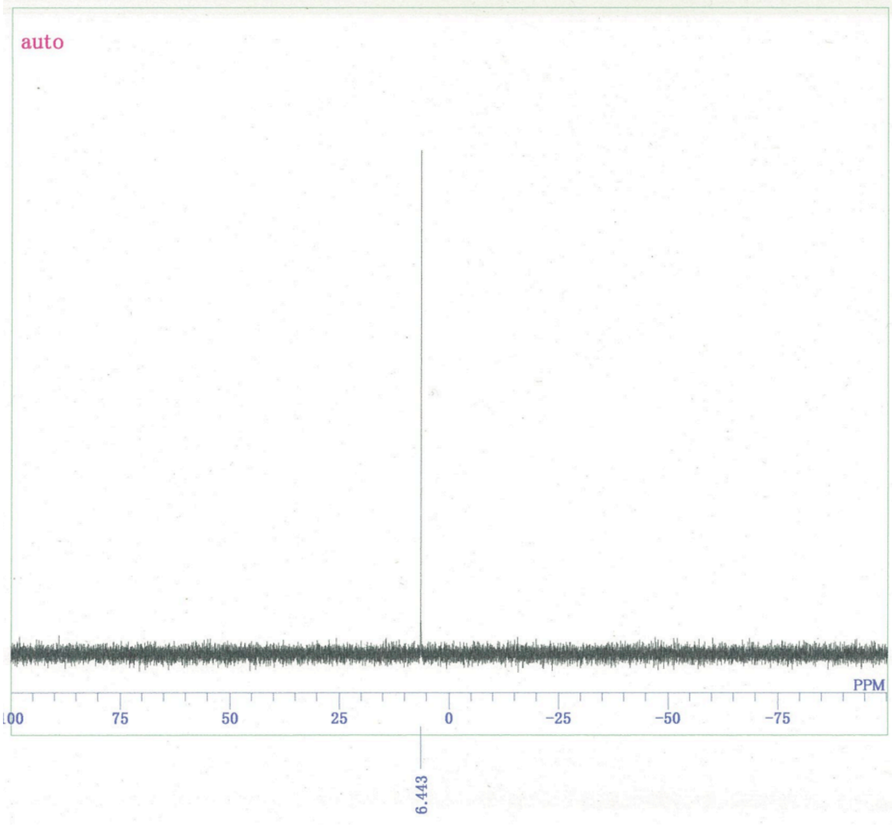

Figure S14. $^{31}P\{^{1}H\}$ NMR spectrum of **5** (162 MHz, CD_3OD).

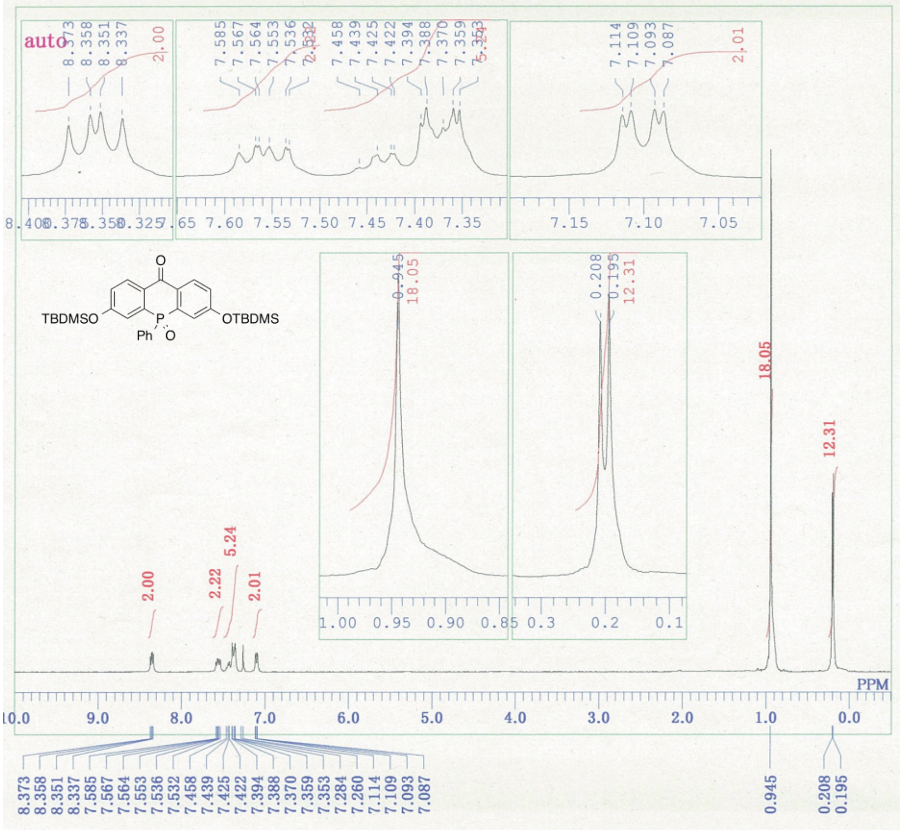

Figure S15. ^{1}H NMR spectrum of **6** (400 MHz, $CDCl_3$).

Figure S16. $^{13}C\{^{1}H\}$ NMR spectrum of **6** (100 MHz, $CDCl_3$).

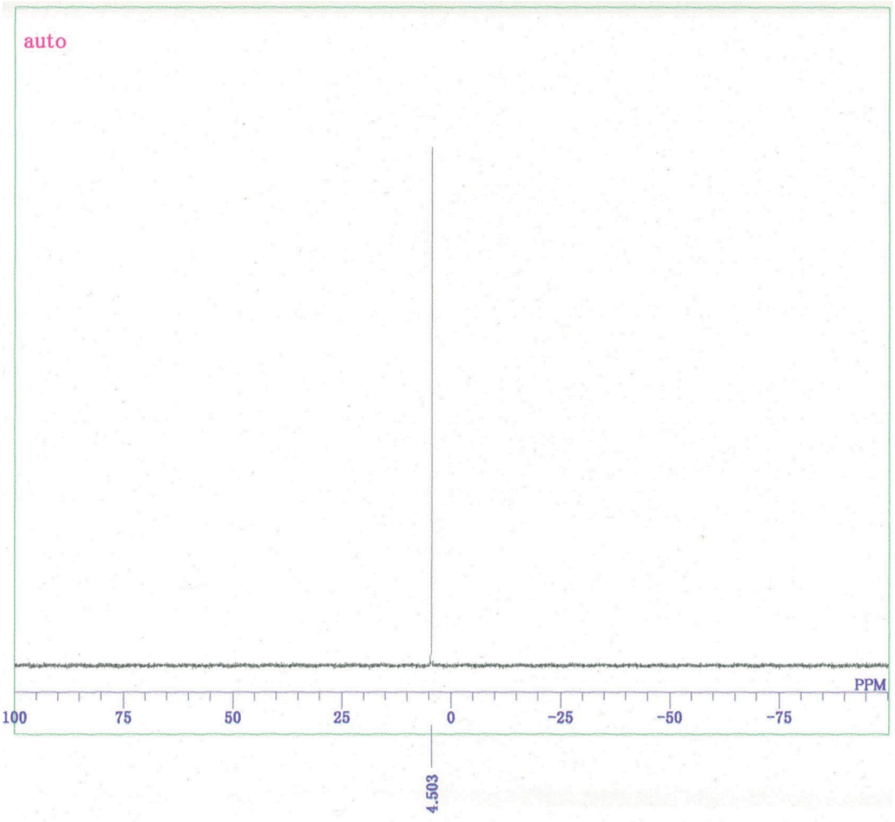

Figure S17. $^{31}P\{^{1}H\}$ NMR spectrum of **6** (162 MHz, $CDCl_3$).

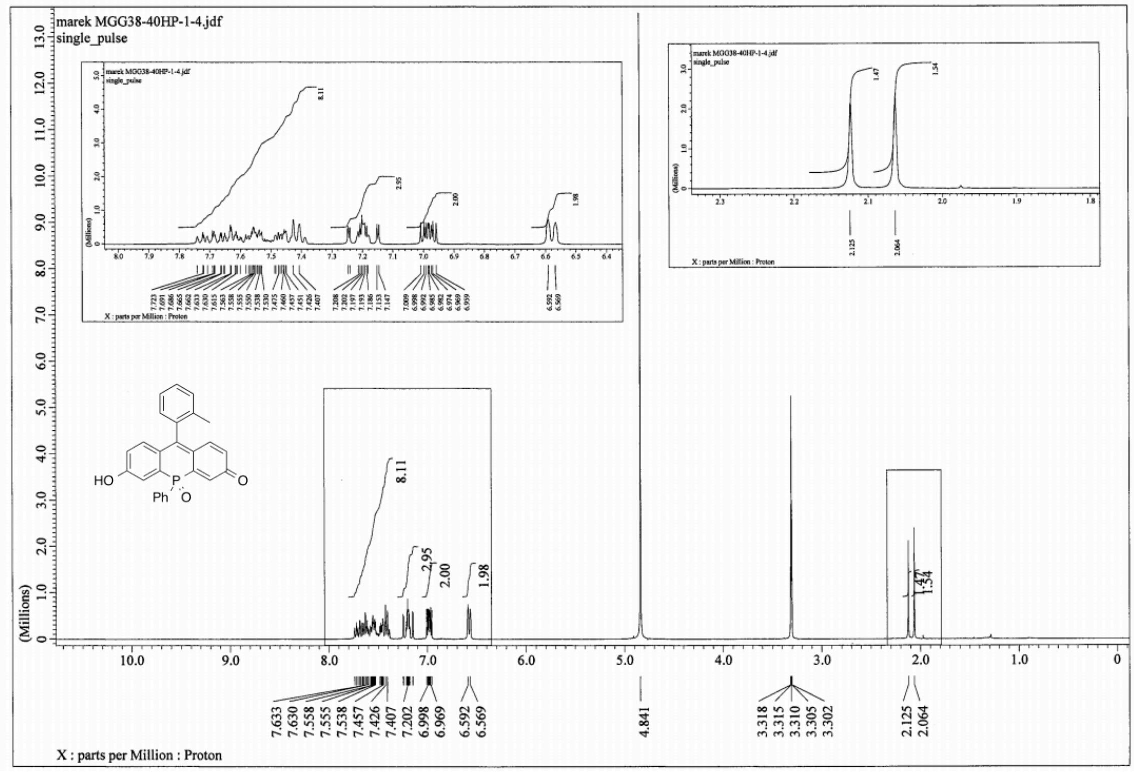

Figure S18. ^{1}H NMR spectrum of **POF** (400 MHz, CD_3OD).

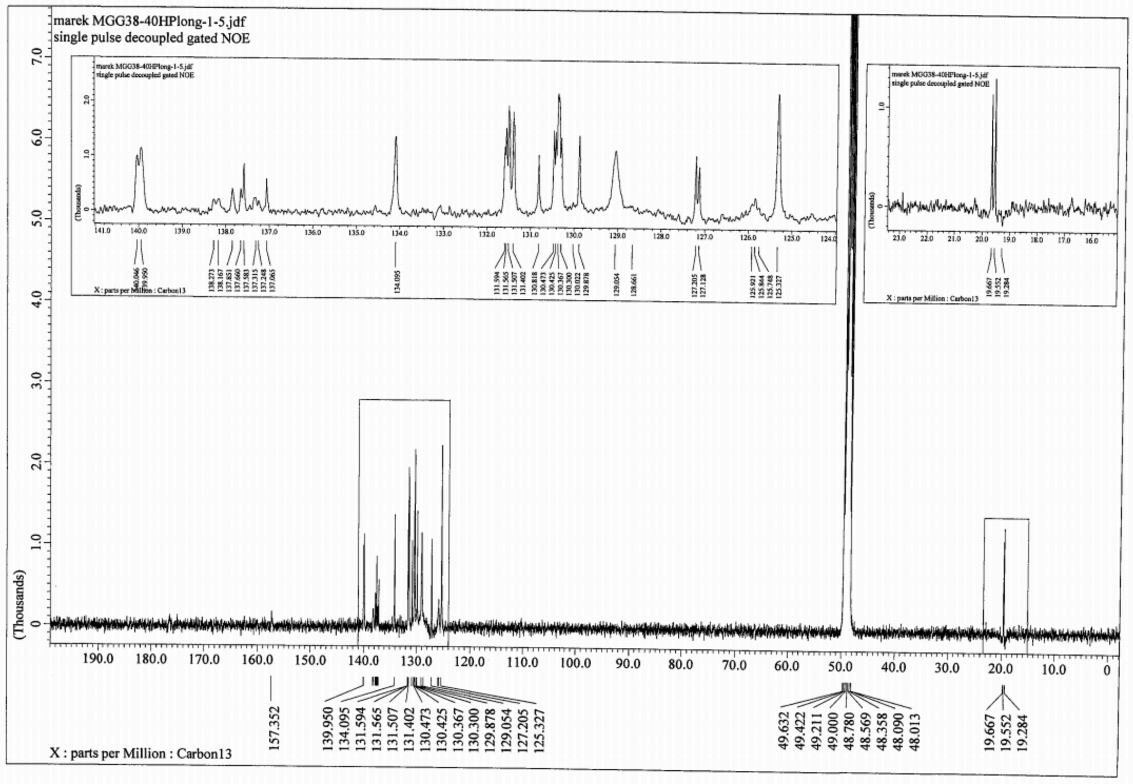

Figure S19. $^{13}C\{^1H\}$ NMR spectrum of **POF** (100 MHz, CD_3OD).

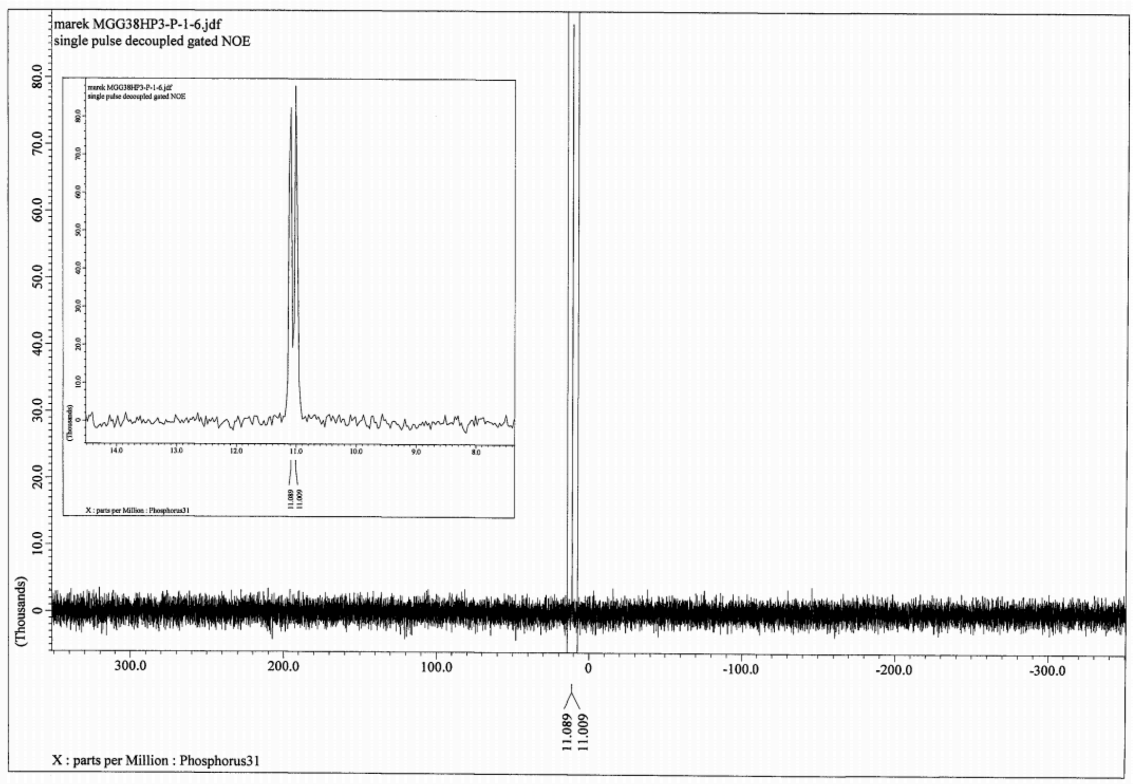

Figure S20. $^{31}P\{^1H\}$ NMR spectrum of **POF** (162 MHz, CD_3OD).

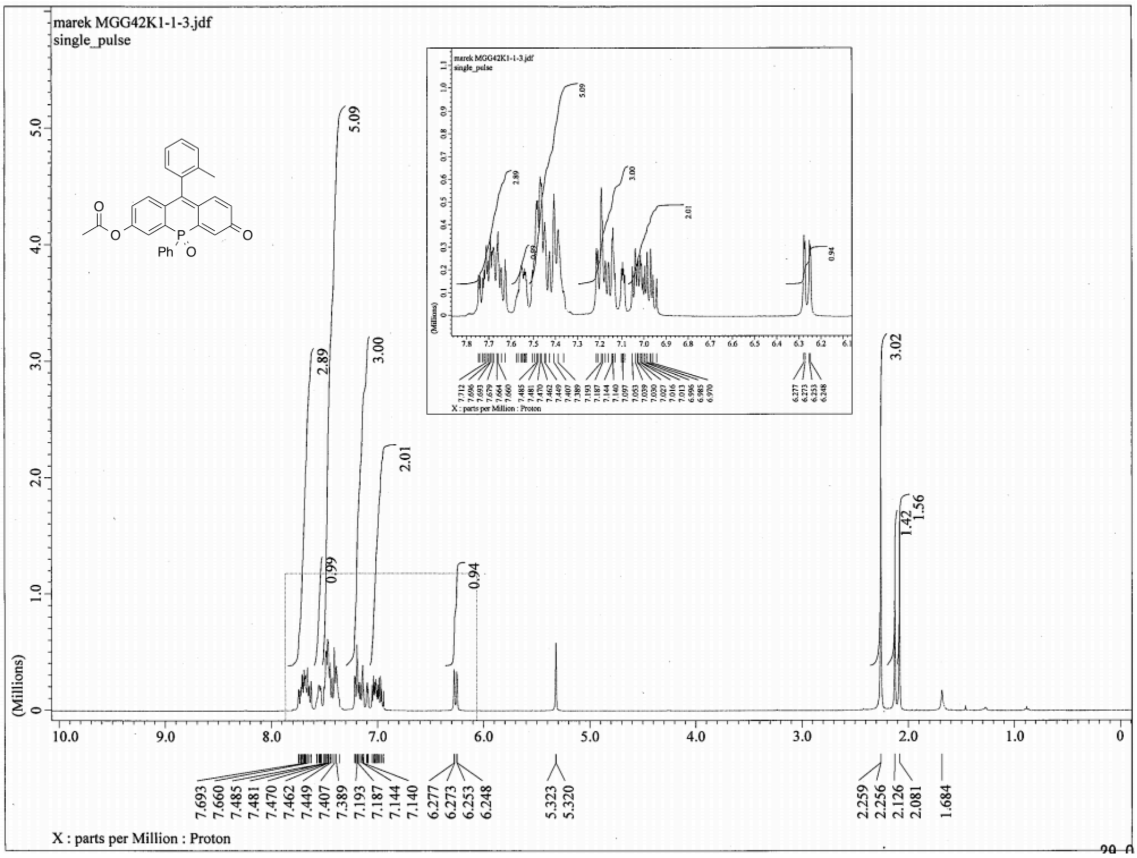

Figure S21. ^1H NMR spectrum of **AcPOF** (400 MHz,CD_2Cl_2).

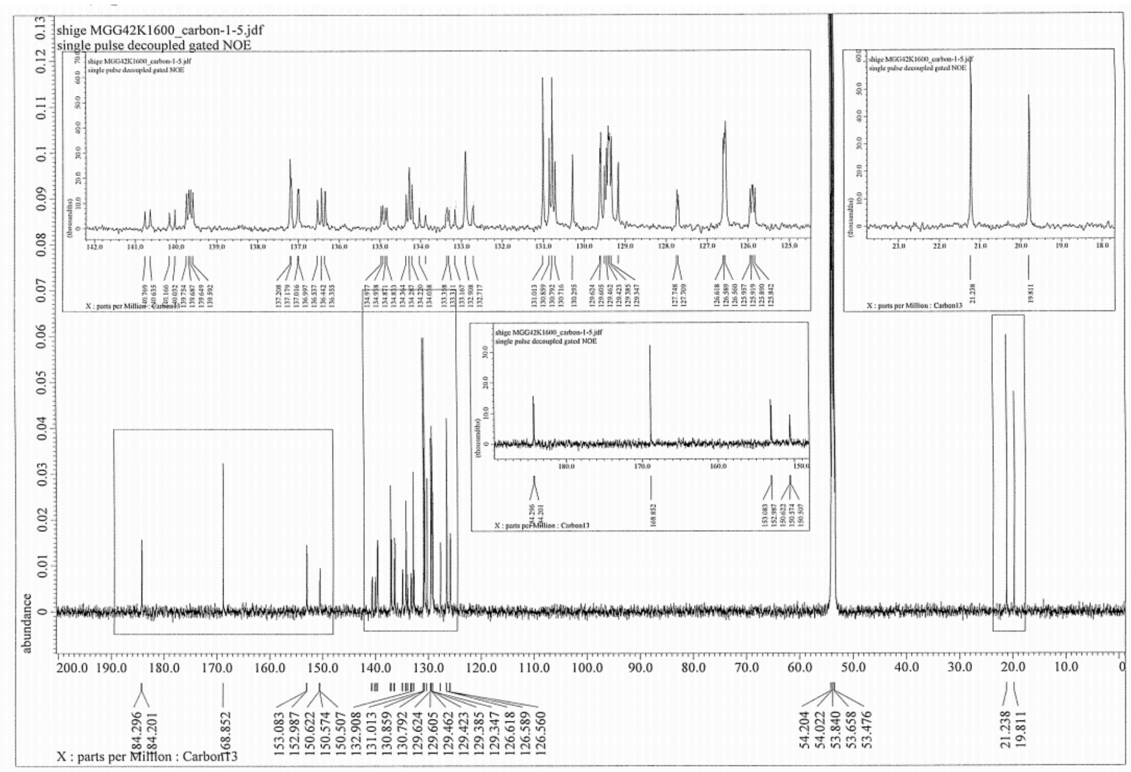

Figure S22. $^{13}C\{^1H\}$ NMR spectrum of **AcPOF** (150 MHz, CD_2Cl_2).

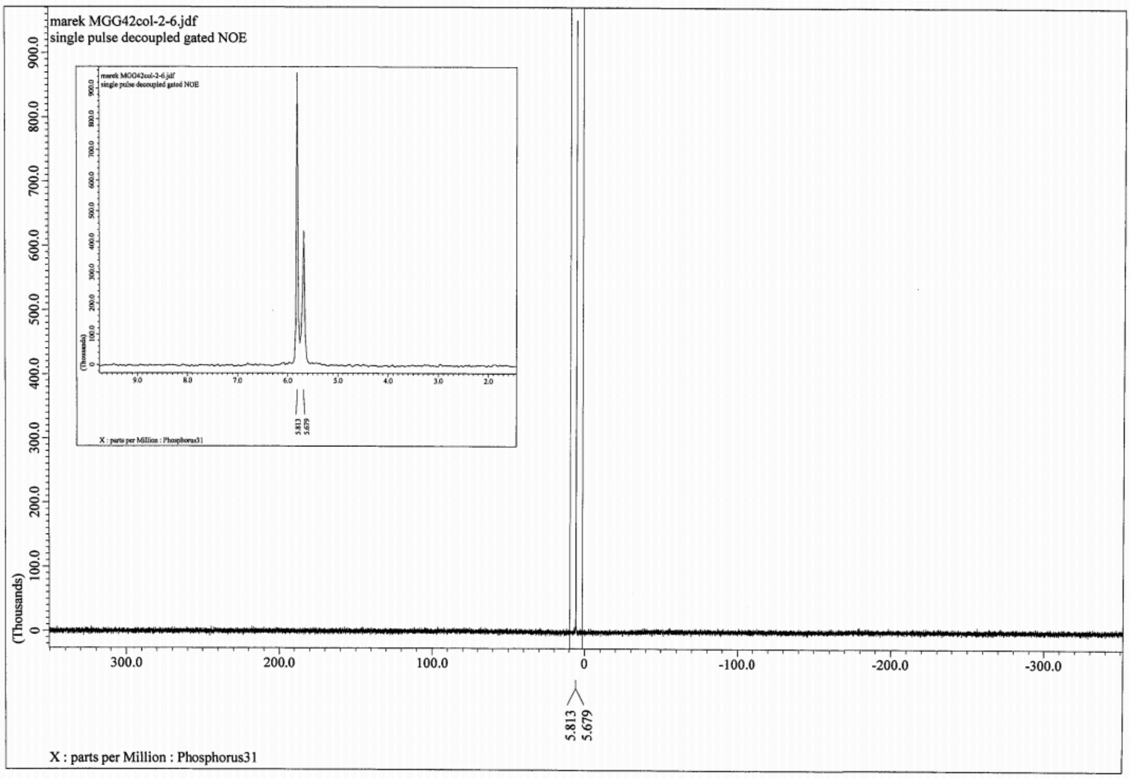

Figure S23. $^{31}P\{^1H\}$ NMR spectrum of **AcPOF** (162 MHz, CD_2Cl_2).